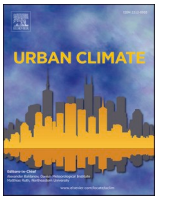
Urban Climate 67 (2026) 102878



Contents lists available at ScienceDirect

Urban Climate

journal homepage: www.elsevier.com/locate/uclim





Post-fire effects on LST and UHI: A remote sensing and GIS assessment

Mehtap Özenen-Kavlak [a], Müzeyyen Anıl Şenyel Kürkçüoğlu [b], Halil Duymuş [c,*], Gülşah Bilge Öztürk [d], Saye Nihan Çabuk [e], Ceren Özcan Tatar [f,g], Alper Çabuk [h,i]

[a] Faculty of Open and Distance Education, Department of Geography, İstanbul University, 34398, Sarıyer, İstanbul, Türkiye.
[b] Faculty of Architecture, Department of City and Regional Planning, Middle East Technical University, 06800 Ankara, Türkiye.
[c] Faculty of Architecture, Department of Landscape Architecture, Çukurova University, 01330 Adana, Türkiye
[d] Faculty of Agriculture, Department of Landscape Architecture, 52200, Ordu University, Ordu, Türkiye
[e] Eskisehir Technical University, Institute of Earth and Space Sciences, Geodesy and Geographical Information Technologies Department, 26555 Eskisehir, Türkiye.
[f] Department of Remote Sensing and Geographical Information Systems, Eskisehir Technical University, Eskişehir, Türkiye.
[g] Basarsoft Information Technologies, Ankara, Türkiye.
[h] Faculty of Architecture and Design, Department of Architecture, Eskişehir Technical University, 26555 Eskisehir, Türkiye.
[i] TAPLAK, Design and Planning Accreditation Association, Eskişehir, Türkiye.

ARTICLE INFO

Keywords:
Forest fire
GIS
LST
Manavgat
RS
UHI

ABSTRACT

The 2021 Manavgat wildfire in Türkiye caused significant alterations in land surface temperature (LST) and the urban heat island effect ratio (UHIER), with spatial variations influenced by proximity to the coast. This study investigates these post-fire thermal dynamics using Landsat 8 satellite imagery analyzed through remote sensing (RS) and geographic information systems (GIS) techniques. The study area was divided into coastal and inland zones to assess the maritime effect. Results show that the LST increased by 2.5 °C to 5 °C across 93% of the inland area and 96% of the coastal area, with inland zones experiencing more pronounced thermal stress. In contrast, the UHIER decreased, reflecting a relatively greater temperature rise in rural areas compared to urban settings. The coastal zone exhibited a moderating influence, mitigating extreme temperature increases. These findings emphasize the critical role of forest fires in altering microclimatic conditions and highlight the importance of spatial differentiation in post-fire resilience assessments.

1. Introduction

Forests provide indispensable ecosystems for various species and have a critical role in climate change since they act both as a source and storage for carbon emissions. The two-fold role of forests in climate change, due to being both the cause and the solution, needs to be handled responsively. Forests themselves are subject to the risks imposed by extreme weather conditions resulting from climate change. The global future is likely to be characterized by modified forest disturbance regimes, while the number, scale and

* Corresponding author.
E-mail addresses: mehtapozenen@eskisehir.edu.tr (M. Özenen-Kavlak), senyel@metu.edu.tr (M.A.Ş. Kürkçüoğlu), hduymus@cu.edu.tr (H. Duymuş), gulsahbilge@odu.edu.tr (G.B. Öztürk), sncabuk@eskisehir.edu.tr (S.N. Çabuk), ceren_ozcan@ogr.eskisehir.edu.tr (C.Ö. Tatar), acabuk@eskisehir.edu.tr (A. Çabuk).

https://doi.org/10.1016/j.uclim.2026.102878
Received 28 April 2025; Received in revised form 14 October 2025; Accepted 23 March 2026
Available online 27 March 2026
2212-0955/© 2026 Elsevier B.V. All rights are reserved, including those for text and data mining, AI training, and similar technologies.

intensity of the disturbances resulting from fires, insects and pathogens are expected to be increased (Seidl et al., 2017). Forest fires, whether natural or human-induced, are among the most common disturbances that not only degrade forest ecology but also have socio-economic consequences (Çolak and Sunar, 2020; Özenen-Kavlak et al., 2020; Junaidi et al., 2021). The subtle balance between the climate and the sustainability of forests can be destroyed by any alterations in the elements, since forests are highly responsive to fluctuations in fuel moisture triggered by alterations in air temperature, relative humidity, and wind speed; therefore, being more vulnerable to the adverse effects of climate change (Çolak and Sunar, 2020). The expected increase in temperatures will result in a decrease in relative humidity and an increase in fuel dryness. The fire risk turns out to be more serious when precipitation drops working as an expediting condition predisposing to a fire. Daniels et al. (2011) claim that the cumulative effects of human land use even exacerbate the ongoing climate change effects when it comes to forest fires.

The Mediterranean temperate climate zone is defined as being sensitive to forest fires, while fire events including mega fires are not uncommon in the region (Kotroni et al., 2020; Daşdemir et al., 2021; Karali et al., 2023). Çolak and Sunar (2023) state that forest fires are becoming more prevalent globally, while the number of fires increased dramatically in the Mediterranean region in 2008–2020 period. Türkiye, as one of the Mediterranean countries, faces significant vulnerabilities when annual forest damage is considered. Both the direct and indirect effects of the fires have various ecological and economic impact in addition to the costs of fire control and prevention (Kalogiannidis et al., 2023). Large wildfires change the albedo and vegetation of a region and affect temperature, weather, and energy balance (Chen et al., 2014), causing greater damage to trees than all the other disturbances that forests face including diseases or insect invasions (Çolak and Sunar, 2020). In addition to such ecological consequences, disruptions in utilities such as energy and transport systems, displacement of people, decline in property values and investments, loss of livelihood and well-being are denoted as the socio-economic costs (Kalogiannidis et al., 2023). Detecting the post-fire impact is also crucial in land-use decisions, continuity of economic activities and restructuring of the infrastructure and built-up areas.

The change in the land surface temperature (LST) and the urban heat island ratio effect (UHIER) are among the environmental consequences of forest fires, although few studies have mentioned such an impact in the literature up to now. Changes in the LST are directly related to land cover and the severity of fire impact, or how much and how deep the surface layer has burned (Veraverbeke et al., 2012). It could also be said that variations in the LST depend on the severity of the fire or burn, as well as the geography and weather (Vlassova et al., 2014). The impact of the fire on the LST and UHIER becomes more important when the affected area include settlements, since the residents would be subject to the long-term effects of the fire as a result of the land cover change and increased heat effect.

The severity and the spatial distribution of the impact of forest fires reflect geographic variations even in the same area, while accounting for that variability would enable the development of precise and timely decision-making and recovery intervention. Currently, as one of the most economic and effective methods for monitoring forest dynamics, regionally or globally, remote sensing provides the ability to identify forest disturbances and map changes in forests, including analyzes to map affected areas after fires (Chen et al., 2014; Ozenen Kavlak et al., 2021).

Satellite retrieved LST can be used for both pre-forest and post-forest fire assessments. Çolak and Sunar (2023) provide evidence for the detection of forest fire risk with the use of the LST retrieved from Landsat 8 and ASTER. Guangmeng and Mei (2004) used a neural network method with MODIS data to generate the LST to evaluate forest fire risk. Matin et al. (2017) also use fire data from MODIS while calculating the forest fire risk index for Nepal. Peng et al. (2007) and Liu et al. (2010) also utilized LST in forest fire risk assessment. In addition to vegetation cover, as the most significant factor in fires, the LST is calculated as the second most important factor particularly in ignition and spread. An advanced Space-borne Thermal Emission and a Reflection Radiometer (ASTER) instrument aboard the Terra satellite are two common space-based systems used today with their thermal infrared (TIR) sensors to determine the LST (Cristóbal et al., 2018; Barraza et al., 2019). Another indication of a risk factor for wildfire is water-related stress in plants, and the LST is an excellent predictor of this (Manzo-Delgado et al., 2009). The normalized difference vegetation index (NDVI) data, used to assess water stress or specifically plant health and density, and the LST, measured by remote sensing, could be compared to ensure the accuracy of the LST within a specific time frame for the area of interest and to address the question of the accuracy of the LST (Sajib and Wang, 2020; Çolak and Sunar, 2023).

Despite the increasing body of research investigating the risk assessment and early detection of forest fires using LST and vegetation indices, the post-fire impacts on UHIER and microclimatic variations have been largely overlooked. In particular, the role of large water bodies such as seas in moderating the post-fire heat stress in affected regions has not been systematically addressed. Moreover, while existing studies have mostly focused on general temperature changes, there is a lack of research distinguishing between urban and rural responses in fire-affected areas. Recent systematic reviews have highlighted the critical importance of understanding the spatial and temporal variations of urban heat island effects in different geographic contexts, emphasizing the need for integrated and differentiated post-fire analyses (Duymuş et al., 2025). Motivated by these gaps, this study aims to evaluate the spatial and quantitative impacts of the 2021 Manavgat wildfire in Türkiye on LST and UHIER patterns, distinguishing between the sea-facing and inland zones. By incorporating Remote Sensing (RS) and Geographic Information Systems (GIS) methodologies, the research offers new insights into the spatial variability of post-fire thermal dynamics, thereby contributing to improved understanding of microclimate resilience in wildfire-prone regions.

The objective of this study is to determine the impact of the LST and UHIER of the 2021 wildfires in the Manavgat region of Antalya, Türkiye, using satellite imagery before and after the fires. Spatial variations in the LST and UHIER are considered while the area is investigated in two separate geographic zones to distinguish the maritime effect. Forest fire prediction using the UHIER and LST are presented in the literature, yet the change in the UHIER and LST after a fire have not been addressed, and this study intends to fill that overlooked research area. The other contribution of the study is utilizing RS and GIS in the analysis of the UHIER and LST changes due to forest fires, with a special emphasis on geographic variations.

2. Material and methods

This section describes the study area, material, and methods used.

2.1. The study area and data

The district of Manavgat is located in the province of Antalya in the Mediterranean region. With an area of 2283 km^2 and a population of more than 230,000 inhabitants, it is the largest district of the Antalya province. It is located in the fertile plain of the Manavgat River. The center of the district is about 3.5 km from the Mediterranean coast. The district is 75 km east of Antalya and 60 km west of the district of Alanya. The historic ancient city of Side is located within the district boundaries (Matso, 2023). In Manavgat district, the altitude varies between 0 and 2499 m, and the slope varies between 0° and 80°. The average elevation and slope of the district are 585 m and 16.56° (Akıncı and Akıncı, 2023). The natural vegetation of the district is maquis. The region has a Mediterranean climate with hot and dry summers and warm and rainy winters. The average temperature varies between 30 and 34 °C in summer and 9–15 °C in winter. The annual average relative humidity is 64%. Only 40–50 days a year are cloudy and rainy (Antalya Büyükşehir Belediyesi, 2021; MGM, 2023). The natural structure of the district is partially suitable for agriculture, and agriculture has developed in these regions. The remaining regions are divided into forest and scrubland areas and villages where livestock farming is practiced. Forestry products and seasonal agricultural work are the main sources of income. In addition, tourism as a natural income for the region is one of the most important sources of income in the district (Matso, 2023).

The Mediterranean Basin is one of the most diverse areas in terms of biodiversity (Cuttelod et al., 2008). According to the conservation priorities defined by Myers et al. (2000), the Mediterranean Basin is also a biodiversity hotspot. Red pine forests (*Pinus brutia*) and maquis formations make up the majority of the vegetation in the Mediterranean region (Seyhan, 1990). The forests of the Manavgat district are managed by the Manavgat Forestry Directorate (Manavgat Orman İşletme Müdürlüğü), which is affiliated to the Regional Forestry Directorate in Antalya. The directorate is responsible for an area of 90,210 ha. 57% of the area (51,671 ha) consists of forest areas (OBM, 2023). The Manavgat wildfire occurred between 28 July and 8 August 2021, lasting approximately 10 days, and

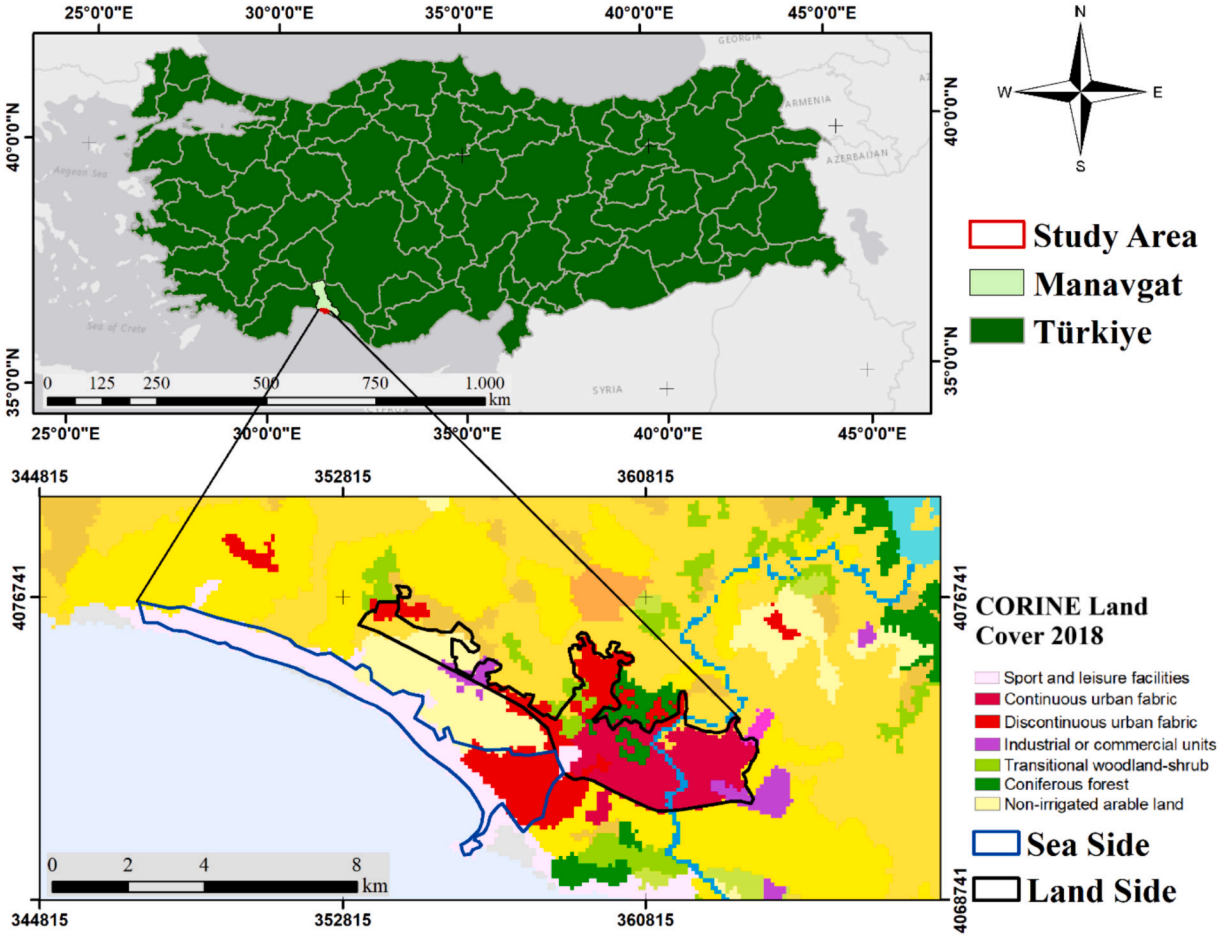


Fig. 1. Study area.

burned an area of about 60,800 ha (Kolukırık et al., 2022; Çinar et al., 2024). According to meteorological observations, strong northeasterly winds (poyraz) affected the Manavgat district on 28–29 July 2021, during which the average hourly relative humidity dropped to as low as 6%, while the air temperature rose to 41 °C (MGM, 2021). The decrease in atmospheric humidity, combined with the drying effect of the winds, caused a rapid decline in the moisture content of dead fuels, which was calculated to have decreased to approximately 3% (Bilgili et al., 2019). Moreover, on 28 July, the Meteorological Fire Index (MYİ) reached a value of 99, with a daily average of 87 (Tovag, 2021). As the event progressed, relative humidity and fuel moisture gradually increased, while wind speed decreased, resulting in a reduced rate of fire spread. On 30 July 2021, areas of high burn severity accounted for approximately 47% of the total burned area (Kırbıyık, 2023). The wildfire, which began on 28 July 2021, affected about 28,327 ha, corresponding to roughly 35% of the forested land within the Manavgat district within just two days (Kavzoğlu, 2021).

The built-up areas of Manavgat and Side are manually delineated through the visual analysis of satellite images. The urbanized area is divided into two sub-areas; the sea side and the land side (Fig. 1) to demonstrate the maritime effect. The Mersin-Antalya Road, which extends in the east-west direction throughout the study area, is considered as a reference in the spatial differentiation of the sea side and the land side.

To compare the situation before and after the Great Manavgat Fire, Landsat 8 satellite images were downloaded from the USGS platform. Detailed information about these images can be found in Table 1. Although the image resolution of the thermal band is 100 m, it is downscaled to 30 m by the data provider before it is made available to users. In order to reduce the impact of seasonal variations, cloud-free Landsat 8 scenes were selected from August 2020 (prior to the fire) and August 2021 (following the fire), which exhibited comparable solar geometry, vegetation phenology, and atmospheric conditions.

All geographical analyzes in the study were carried out using the ArcGIS 10.8.2 program.

2.2. Method

The main method used in the study is based on the image and statistical analysis of satellite images in a GIS environment.

After this, the LST and UHIER were calculated using Landsat 8 OLI images for before and after the Great Manavgat Fire in 2021. The calculated LST and UHIER data was divided into five classes and mapped. In addition, the LST and UHIER differences between 2020 and 2021 were calculated and mapped on unclassified maps. These maps were created in the GIS environment by extracting the 2020 maps from the 2021 maps using the raster calculator tool.

2.2.1. The LST

The LST is a measure of the radiative temperature of the Earth's surface. It is calculated using remote sensing data, such as satellite images, and is influenced by various factors, including vegetation cover, land use/land cover (LULC), and climate conditions (Gelata et al., 2023; Hussain et al., 2023). The LST is an important parameter in understanding the Earth's energy balance, the UHIER effects, and the climate change impact (Goldblatt et al., 2021).

In the context of the LST calculation, RS data/techniques, such as thermal sensors onboard satellites, are used to estimate the LST. These data are then processed and analyzed using GIS tools to understand the spatial distribution and temporal changes of the LST in a given area (de Almeida et al., 2021). Vegetation indices, such as the NDVI, are often used in conjunction with the LST to study the relationship between vegetation cover and surface temperature. The NDVI is a measure of the greenness or health of vegetation and can provide insight into the availability of water and energy in an ecosystem (Gelata et al., 2023). Eq. (1) below is used for calculating the NDVI values (Kumar et al., 2022).

$$\mathrm{NDVI} = (NIR - RED)/(NIR + RED) \tag{1}$$

The method for calculating the LST is given in Table 2.

2.2.2. The UHIER

The UHIER is a phenomenon where urban areas experience higher temperatures than surrounding rural areas due to human activity, such as transportation, industry, and building (Heaviside, 2020). The UHIER can be quantified using various indices, including the urban-rural temperature difference, the UHI intensity (UHII), and the UHI magnitude (UHIM) (Rizwan et al., 2008). The UHIER can be calculated using remote sensing and GIS technology (de Almeida et al., 2021). For the UHIER analysis, an LST analysis of the study area should first be performed. After this, the UHIER value is calculated by subtracting the average LST of rural areas from the LST value of pixels (Eq. 2) (Huang et al., 2019a).

Table 1
Information about the Landsat 8 satellite images used in the study.

Date of image capturing	Situation	Scene center time	Bands used in the study	Wavelength (micrometers)	Resolution (meters)
13.08.2020	Before fire		Band 10 - Thermal Infrared (TIRS) 1	10.6–11.19	100 (30)
		08:28	Band 4 - Red	0.64–0.67	30
			Band 5 - Near Infrared (NIR)	0.85–0.88	30
16.08.2021	After fire		Band 10 - Thermal Infrared (TIRS) 1	10.6–11.19	100 (30)
		08:28	Band 4 - Red	0.64–0.67	30
			Band 5 - Near Infrared (NIR)	0.85–0.88	30

Table 2
The formulas used in the calculation of the LST (Kumar et al., 2022).

Analysis	Formula	Definition
Top of atmospheric reflectance (TOA)	TOA (L) = $ML * Qcal + AL$	ML = Radiance multiplicative Band (no.10) Qcal = Quantized and calibrated standard product pixel values (DN). AL = Radiance Add Band (no.10)
Brightness Temperature (BT) (°C)	$BT = K_2 / (\ln((K_1/L) + 1)) - 273.15$	K_1, K_2 = constants for the thermal band, L = the TOA radiance value. To obtain the results in Celsius, the radiant temperature is adjusted by adding the absolute zero (approx. −273.15 °C)
Proportion of vegetation (Pv)	$Pv = ((NDVI - NDVI_{min})/(NDVI_{max} - NDVI_{min}))^2$	The minimum and maximum values of the NDVI image
Land surface emissivity (ε)	$\varepsilon = 0.004 * Pv + 0.986$	The value of 0.986 corresponds to a correction value of the Equation.
LST	$LST = (BT / (1 + (\lambda * BT / C2) * Ln(\varepsilon)))$	λ = Wavelength of emitted radiance (0.00115) C2 = the constant (14,388 μm K)

$$UHIER = \Delta Ti/Ts = (Ti - Ts)/Ts \quad (2)$$

Ti = The LST of the i-th pixel.

Ts = The mean LST of rural lands

In order to better understand and discuss the UHIER, different approaches are used to assess the UHI intensity. In this study, the UHIER index is used to investigate the quantitative differences in the Surface Urban Heat Island (SUHI) between rural and urban areas. The use of UHIER in this study is preferred over the conventional UHII because it provides a normalized comparison based on surface temperatures retrieved from satellite imagery, offering a more accurate representation of spatial thermal variations post-fire. The primary index was developed as the UHI Ratio Index (URI) by Xu and Chen (2004) and modified for other studies. The UHIER formula in this study is based on the research of Huang et al. (2019a, 2019b), which explains the UHIER as the relative LST investigation.

The UHIER values obtained by applying the above-mentioned procedures are usually classified into different categories considering the minimum and maximum values in the study areas (Li and Yin, 2013; Zhang et al., 2013; Huang et al., 2019b). Each category refers to the amount of the LST difference between urban and rural areas. The negative values indicate the areas where urban land temperatures are lower than rural land temperatures, and the positive values indicate the warmer urban areas compared to the surrounding rural areas. Consequently, increasing negative values are associated with the gradually decreasing LST values in urban areas compared to rural areas, while increasing positive values show the degree of the increased LST in the urban fabric. As the values approach 0, the difference between the compared areas decreases.

The UHIER values for the study areas in 2020 and 2021 range between 0.17 and − 0.25 and were divided into five equal ranges; highly cooler, moderately cooler, slightly cooler, slightly warmer, and moderately warmer (Table 3).

3. Results

Against the background of the information explained in the method section, this section presents the results obtained before and after the Great Manavgat Fire. The results of the study are presented in two separate sections; sea side and land side. The study found that the average LST values used to calculate the UHIER value for land side rural areas are 37.74 °C for 2020 and 44.097 °C for 2021. It is noteworthy that the mean LST value in the rural inland region had increased by about 6 °C, which is due to the bare areas without trees after the large forest fire.

3.1. The sea side

The maps in Fig. 2 were created as a result of the analyses carried out for the sea side. It was found that the LST values of 2020 vary between 33 °C and 42 °C, and the LST values of 2021 vary between 33 °C and 43 °C. The resulting maps were divided into five evenly distributed classes, and the LST maps in Fig. 2-a were created. Looking at the LST maps for 2021, an increase in temperature values can be seen in the northeast of the study area. An investigation of the UHIER values in the study area revealed values between −0.12 and 0.11 for 2020 and between −0.23 and − 0.021 for 2021. A classification of the UHIER maps, considering the literature, results in the UHIER map in Fig. 2-b. Accordingly, despite the significant increase in the LST values, a decrease in the UHIER values can be observed, especially in the south of the study area. This situation can be explained by the decreasing effect of the UHIER effect of the sea,

Table 3
The UHIER categories in the study area (Based on the approach of Li and Yin, 2013; Zhang et al., 2013; Huang et al., 2019b).

UHI Value (Level °C)	Level	Explanation
(−0.25) - (−0.17)	Highly cooler	The LST value in the urban area is highly cooler than in the rural area
(−0.17) - (−0.085)	Moderately cooler	The LST value in the urban area is moderately cooler than in the rural area
(−0.085) - (0)	Slightly cooler	The LST value in the urban area is slightly cooler than in the rural area
(0)–(0.085)	Slightly warmer	The LST value in the urban area is slightly warmer than in the rural area
(0.085)–(0.17)	Moderately warmer	The LST value in the urban area is moderately warmer than in the rural area

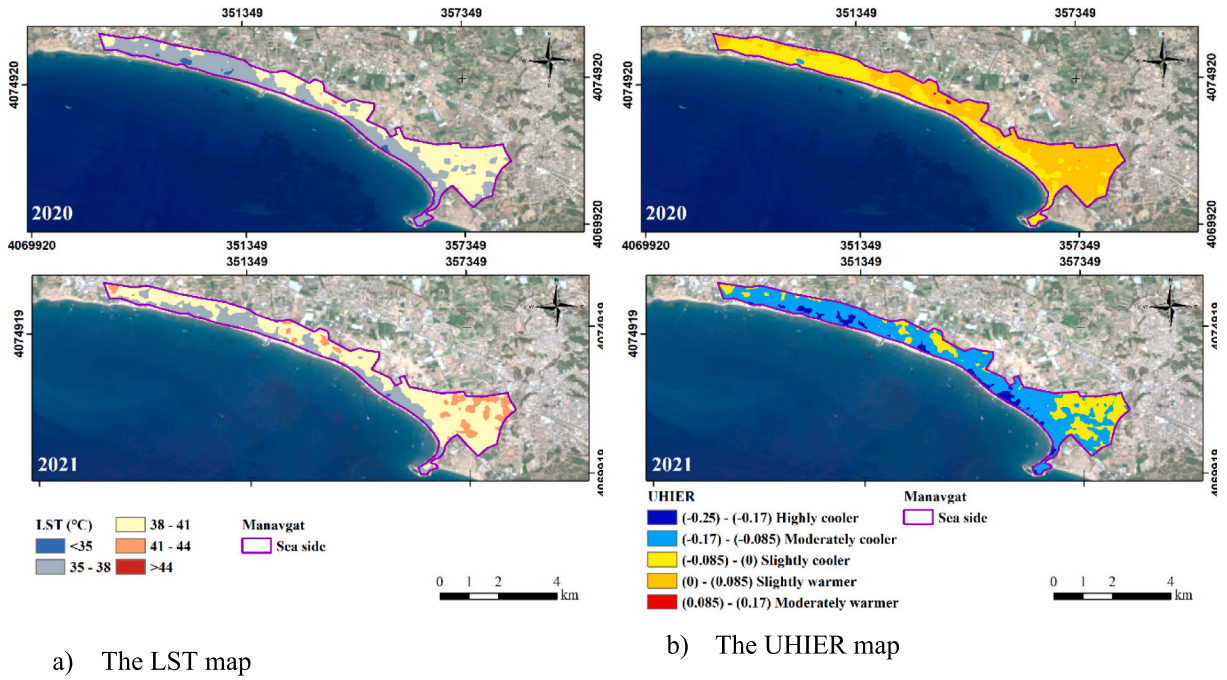


Fig. 2. The LST and UHIER map of the sea side.

depending on the distance of the area from the sea. Moreover, although LST values increased in 2021 compared to 2020, the UHIER values decreased because rural areas experienced a greater temperature rise than urban zones, leading to a smaller urban–rural temperature difference.

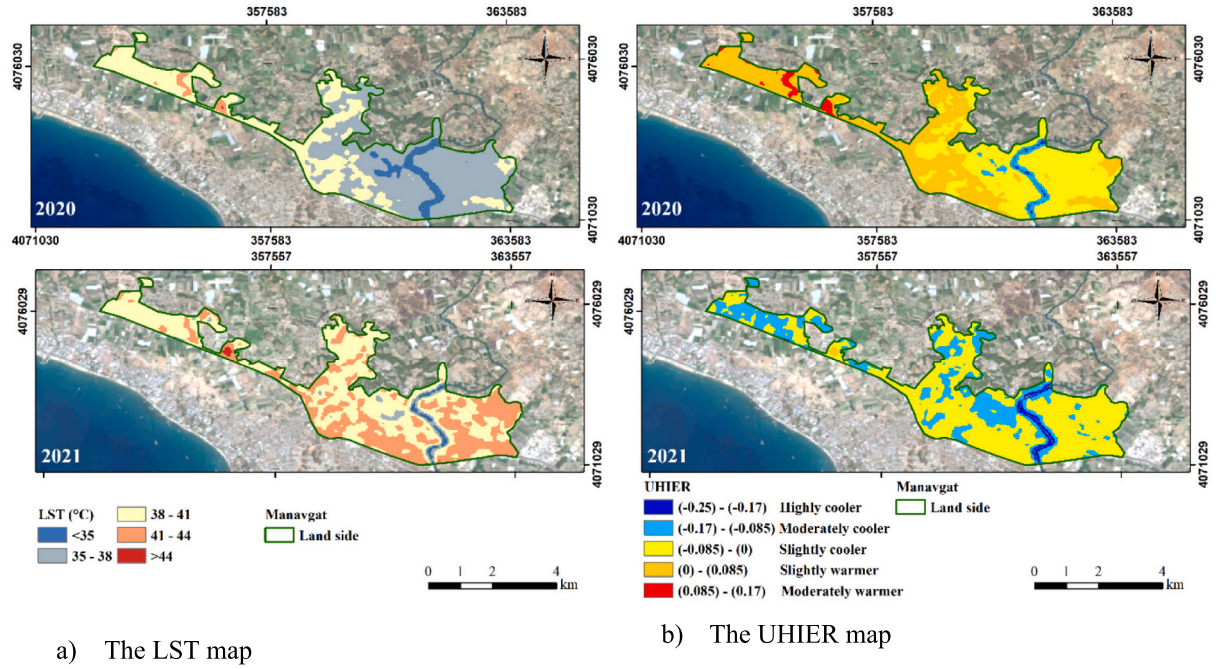
The table showing the areas of these regions in hectares and their percentage distribution can be found below (Table 4). When examining the spatial distribution of the LST values, it can be seen that only two hectares of the area was between 41 and 44 °C before the fire, while one hundred and twenty hectares of the area had these temperature values after the fire. It was found that, in contrast to the LST values, there was a decrease in the UHIER values in the post-fire period.

3.2. Land side

The maps shown in Fig. 3 were created as a result of the analyzes carried out for inland areas. It was found that the LST values for 2020 vary between 30 °C and 44 °C and the LST values for 2021 vary between 33 °C and 46 °C. The resulting maps were divided into equal intervals and the LST maps are shown in Fig. 3-a. Looking at the LST map for 2021, it is clear that the temperature values are increasing in a large part of the study area. When looking at the UHIER values, values between −0.2 and 0.17 were found in the study area for 2020 and between −0.25 and 0.03 for 2021. The classification of the UHIER maps into equal intervals resulted in the maps in Fig. 3-b. This shows that the significant increase in the LST values after the fire in the general area has led to a decrease in the UHIER values in the land region of the study area. This is because rural areas experienced a greater temperature rise than urban zones after the wildfire, primarily due to the loss of vegetation cover and increased surface exposure, which reduced evapotranspiration and enhanced heat absorption. Consequently, the temperature contrast between urban and rural areas decreased, resulting in lower UHIER values.

Table 4
Spatial distribution of the reclassified maps (sea side).

		2020				2021			
		Area (ha)	Percent (%)	Mean	SD	Area (ha)	Percent (%)	Mean	SD
LST (°C)	<35	20	2	37.8	1.34	4	0	39.1	1.63
	35–38	507	50			268	26		
	38–41	492	48			629	62		
	41–44	2	0			120	12		
	>44	–	–			–	–		
UHIER	(−0.25) - (−0.17) Highly cooler	–	–	0.001	0.035	76	7	−0.112	0.036
	(−0.17) - (−0.085) Moderately cooler	6	1			688	68		
	(−0.085) - (0) Slightly cooler	448	44			258	25		
	(0)–(0.085) Slightly warmer	564	55			–	–		
	(0.085)–(0.17) Moderately warmer	2	0			–	–		



a) The LST map

b) The UHIER map

Fig. 3. The LST and UHIER maps of the land side.

Table 5 provides an overview of the spatial distribution of the LST and UHIER maps for inland areas in hectares and percentage. Examination of the spatial distribution of the LST values shows that only three hectares of the area before the fire were between 41 and 44 °C, while five hundred and ninety-three hectares of the area after the fire had these temperature values. For the UHIER values, it was observed that the slightly and moderately warmer areas (2020–716 ha) decreased to only five hectares in 2021.

3.3. *Difference maps*

The LST difference maps created to see the change in the LST distribution in the Manavgat region before and after the large forest fire are shown in Fig. 4. As can be seen in Fig. 4, the impact of the large forest fires on the LST inland is clearly visible. In the east of the region in particular, the increase in the LST is more than 2.5 °C and can exceed 5 °C in a number of places. The observed post-fire increase in land surface temperature can be attributed to the destruction of vegetation cover, leading to reduced evapotranspiration and increased absorption of solar radiation due to the lower surface albedo of burned areas.

Table 6 shows the changes in the study area in terms of area and percentage. It is noteworthy here that the sea effect has a cooling effect on the LST. In the coastal region, the LST change remained between 0 and 2.5 °C in eighty-eight of the areas. In the inland area, the LST increase is between 2.5 and 5 °C in 68% of the areas.

The UHIER difference maps created to see the change in the UHIER distribution before and after the Great Forest Fire are shown in Fig. 5. As can be seen in Fig. 5, the effects of large wildfires on the UHIER, unlike the LST, can be observed on the sea side. The UHIER has changed towards 'moderately cooler' over most of the sea side. The UHIER change, especially in the eastern part of the land side, falls into the 'slightly cooler' category. The increase in the LST generally observed in the region is accompanied by a decrease in the

Table 5
The spatial distribution of the reclassified maps (land side).

		2020				2021			
		Area (ha)	Percent (%)	Mean	SD	Area (ha)	Percent (%)	Mean	SD
LST (°C)	<35	87	6	37.7	1.71	16	1	40.6	1.39
	35–38	839	55			57	4		
	38–41	565	37			854	56		
	41–44	33	2			593	39		
	>44	0	0			5	0		
UHIER	(−0.25) - (−0.17) Highly cooler	4	0	−0.002	0.045	35	2	−0.080	0.031
	(−0.17) - (−0.085) Moderately cooler	60	4			473	31		
	(−0.085) - (0) Slightly cooler	744	49			1.012	67		
	(0)–(0.085) Slightly warmer	680	45			5	0		
	(0.085)–(0.17) Moderately warmer	36	2			–	–		

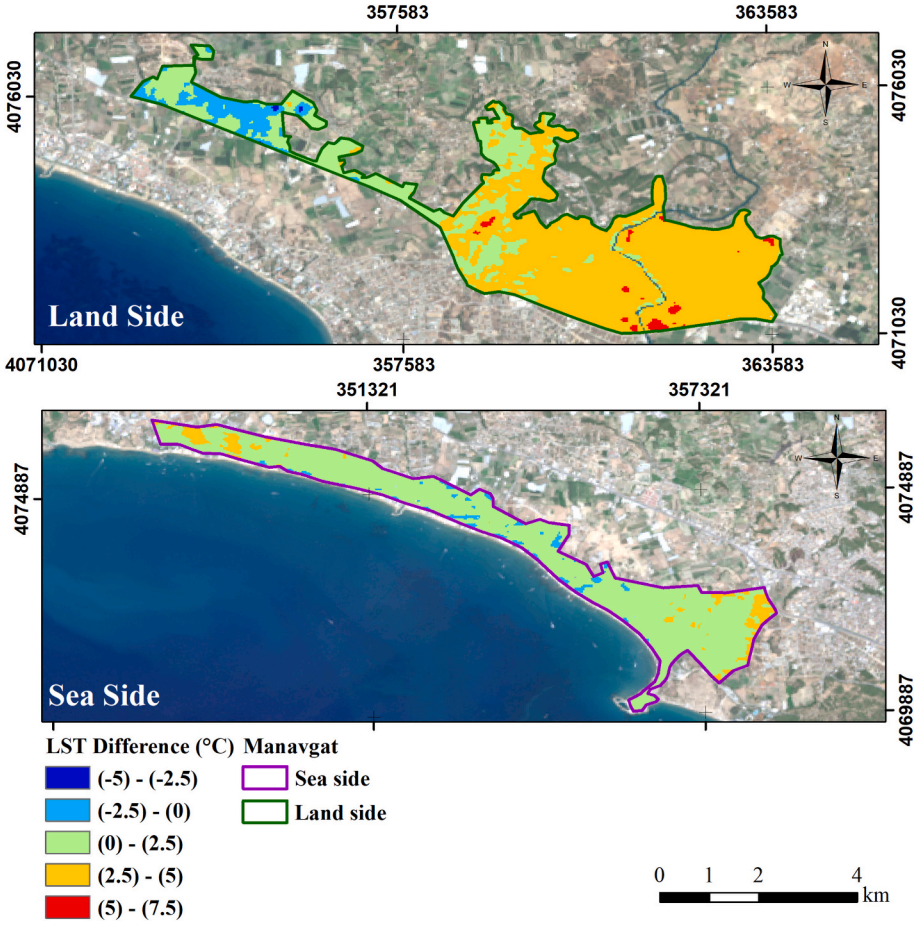


Fig. 4. Maps of the LST difference in the Manavgat region.

Table 6
Change in LST values.

LST Difference (°C)	Sea side		Land side	
	Area (ha)	Percent (%)	Area (ha)	Percent (%)
(−5) - (−2.5)	–	–	2	0
(−2.5) - (0)	44	4	98	6
(0)–(2.5)	893	88	373	25
(2.5)–(5)	85	8	1.030	68
(5)–(7.5)	–	–	21	1

UHIER values. The LST average of the urban and rural areas is used for the UHIER calculations. This formula can be used to calculate the intensity of the temperature difference between the urban and rural areas. It was found that the overall decrease in the UHIER values on both the sea side and the land side is due to a strong change in the LST average in the rural areas, especially the increase after the fire. The decrease in UHIER values after the wildfire indicates that the temperature rise in rural areas was relatively greater than that in urban areas, effectively narrowing the urban–rural temperature differential and thereby weakening the UHIER. When the UHIER density increases to negative values, the urban areas are considered cooler than the rural areas, and when the UHIER intensity increases to positive values, the urban areas are considered warmer than the rural areas. In this study, it is assumed that forest fires lead to a decrease in the UHIER values in the urban areas due to high LST values in the rural areas.

Table 7 shows the effects of the UHIER change in the study area in terms of area and percentage. As can be seen from the table, the sea effect had a more cooling effect on the UHIER than the land side, and a decrease in the UHIER values was observed throughout the area. 94% of the area changed to moderately cooler values. On the land side, the UHIER values changed to slightly cooler values in 65% of the area and to moderately cooler values in 34% of the area.

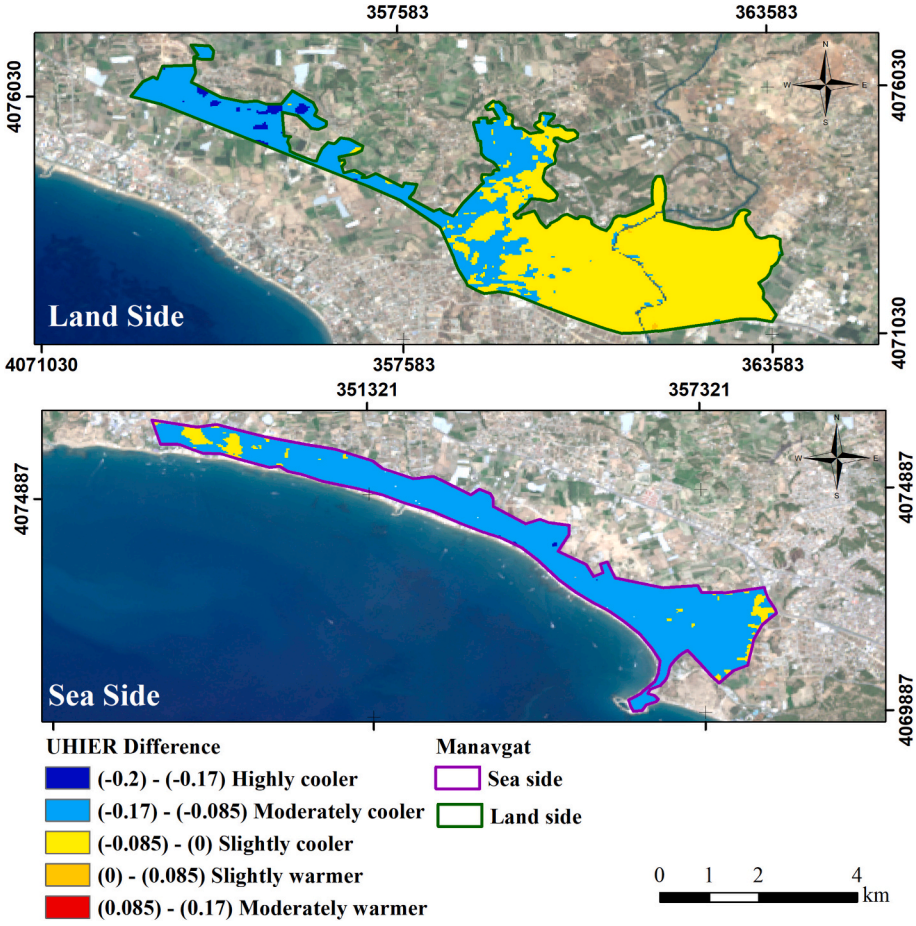


Fig. 5. UHIER difference maps of the Manavgat Region.

Table 7
Change in the UHIER values.

UHIER Difference	Sea side		Land side	
	Area (ha)	Percent (%)	Area (ha)	Percent (%)
(−0.25) - (−0.17) Highly cooler	3	0	19	1
(−0.17) - (−0.085) Moderately cooler	954	94	515	34
(−0.085) - (0) Slightly cooler	64	6	989	65
(0)–(0.085) Slightly warmer	–	–	1	0

4. Discussion

The study aligns with the literature (Guangmeng and Mei, 2004; Peng et al., 2007; Liu et al., 2010; Chen et al., 2014; Matin et al., 2017; Çolak and Sunar, 2020, 2023; Ozenen Kavlak et al., 2021) in demonstrating the effectiveness of using RS and GIS techniques for detecting and mapping the various impacts of forest fires. The main contribution of the study is the investigation of changes and spatial variability in LST and UHIER in relation to forest fires. Although there are studies regarding the detection of forest fire risks through LST (Guangmeng and Mei, 2004; Peng et al., 2007; Liu et al., 2010; Matin et al., 2017; Çolak and Sunar, 2023), the impacts of forest fires on LST and UHIER impacts have been largely overlooked. Among the few studies considering post-fire impacts, the findings of Veraverbeke et al. (2012) and Vlassova et al. (2014) aline with this study, indicating an increase in LST after the fire incident. Similar patterns have been reported in previous studies, where forest fires induced substantial increases in LST and modified local thermal regimes (Veraverbeke et al., 2012; Vlassova et al., 2014). However, this study uniquely distinguishes the maritime influence and spatial variability between coastal and inland zones. Regarding the spatial variability of post-fire impacts, these studies suggest that changes in LST depend on land cover type and fire burn severity. In the case of Manavgat, the land cover effect is examined in relation to the distance from the sea, as well as distinguishing the area into urban and rural.

The results show that the vegetation loss after a forest fire affects not only the forest itself but also the neighboring settlements due to the changes in the LST and UHIER values. The coastal proximity provided a thermal buffer effect, moderating the extent of temperature increases through the high heat capacity of the water body, which delayed and diminished heat accumulation compared to inland areas. The geographic variations in the LST and UHIER changes are clearly observed since the area has a diverse microclimate due to the sea. When the changes in the LST and UHIER are investigated before and after the fire in general, both the increases and decreases are observed at different levels. The most remarkable outcome is that the LST tended to increase whereas the UHIER tended to decrease overall for both the sea and land areas after the forest fire. This pattern indicates that the temperature increase in rural areas was more pronounced than in urban areas, thus narrowing the urban–rural temperature gap and reducing the UHIER values despite the overall LST rise. Here, it is important to note that the definition of the UHIER is based on the comparison of temperatures between urban areas and their surrounding rural counterparts. The absolute value of LST increases across the entire area, regardless of whether it is urban or rural. However, the relative increase in the temperature is higher in rural areas compared to urban areas, resulting in a decrease in the UHIER following the fire incident.

When the results are investigated in detail, it is observed that while the LST values between 38 °**C** and 44 °C covered 48% of the area in 2020, this rate increased to 74% in 2021 in the sea part. The highest LST group, 41 °**C**–44 °**C**, being negligible in 2020 with two hectares, covered one hundred and twenty hectare area in 2021, which refers to 12% increase. The surface temperatures increased up to 2.5 °C in 88% of the sea area while 8% of the entire sea area experienced a surface temperature increase between 2.5 °C and 5 °C. On the contrary, correspondingly the UHIER values decreased while slightly warmer and moderately warmer areas, the highest two UHIER groups, totally disappeared in 2021. Moderately and slightly cooler areas covered 45% and slightly warmer areas covered 55% of the sea area in 2020, whereas all of the UHIER classes fall into cooler groups in 2021.

LST increases in the land area are greater than those in the sea area, while the decrease in the UHIER is comparatively lower. The 38 °C–44 °C LST value group, which had covered 39% of the total in 2020 area, increased to 95% in 2021. The highest LST group turned out to be 44 °**C** and higher in 2021, which covered 5 ha. The largest LST group, which had been 35 °**C** -38 °**C** in 2020 turned out to be 38 °**C** -41 °**C** in 2021, both making up slightly more than half of the total land area. At that point, it is important to note that the surface temperature increases between 5 °C and 7 °C were observed in the land area, although these increases occurred in a very small region. %68 of the entire land area witnessed 2.5 °C to 5 °C increase. Contrary to this, the UHIER tended to fall. The UHIER values in the cooler groups covering 54% of the area in 2020 covered the whole area with no warmer UHIER groups being observed in 2021.

When comparing the observed LST increases following forest fires to figures reported in the literature, the findings of this study are lower than those of other studies. Çolak and Sunar (2020) reported an LST increase ranging from 1 °C to 11 °C, while Vlassova et al. (2014) observed an average increase of 7.6 °C. Veraverbeke et al. (2012) reported a mean increase of 8.4 K in daytime LST, which is considered as an equivalent of 8.4 °C as it represents a temperature difference. In this study, an LST increase of 0 °C to 5 °C LST was observed in 96% of the sea area and 93% of the land area, with an additional 1% of the land area experiencing an increase of 5 °C -7.5 °C. The potential mitigating influence of the large water body may have contributed to these results.

When the impact of proximity to the sea is investigated through a comparison of the sea area and the land area, variations in the LST and UHIER values are also observed. The average LST values tend to be lower in the sea part which is thought to result from the cooling effect of the water body. However, the percentage decreases in the lower LST groups and the percentage increases in the higher LST groups are more pronounced in the land area, which demonstrates the mitigating role of the sea under extreme weather conditions. For instance, the increase in the land area is 37% while it remains 12% in the sea area for the highest LST group (41–44). However, in the UHIER change, the findings indicate that the percent changes are more prominent in the sea area, which also results from the cooling effect of the water body. The temperature increases in the urban and the rural areas alike in the land area whereas the alleviating effect of the sea helps with the cooling of the rural areas more than the built-up areas, resulting in a higher difference in the UHIER values of both urban and rural. The only exception is the moderately warmer areas which covers a negligible area in the sea part, where no change is observed.

Recent studies emphasize that post-fire changes in LST and urban UHIER vary significantly depending on land cover types and topographic conditions. Jodhani et al. (2024a, 2024b, 2024c) demonstrated that forest fires cause notable increases in LST values, particularly in arid and semi-arid environments, by utilizing multi-temporal satellite analyses with Google Earth Engine. Likewise, Jodhani et al. (2024a, 2024b, 2024c) highlighted that LULC alterations, such as the transition from forested areas to barren or urban surfaces, significantly affect local thermal dynamics and environmental quality.

The results of the present study are consistent with these findings, showing a 2.5–5 °C increase in LST in most inland and coastal areas following the 2021 Manavgat wildfire. These results reinforce the understanding that forest fire impacts are not spatially uniform but are modulated by proximity to water bodies and pre-fire land cover characteristics. This study offers significant contributions to the fields of remote sensing and geographic information systems by providing a spatially explicit assessment of post-wildfire thermal dynamics using freely available satellite datasets. By distinguishing between coastal and inland zones, the research advances current understanding of the moderating influence of large water bodies on post-fire LST and UHIER patterns. The integration of UHIER as a normalized metric enhances comparative analyses between urban and rural areas, offering a replicable methodology for post-disaster environmental monitoring. These insights are critical for researchers, urban planners, and disaster resilience professionals aiming to develop spatially targeted adaptation and mitigation strategies in wildfire-prone coastal regions.

This study has several limitations that should be acknowledged. Firstly, the spatial resolution of the satellite data used (Landsat 8 and MODIS) may not fully capture micro-scale variations in surface temperature and land cover changes. Secondly, while the analysis effectively distinguished coastal and inland thermal dynamics post-fire, meteorological parameters such as wind speed, humidity, and precipitation were not explicitly incorporated, which could further influence the surface thermal responses. Thirdly, to ensure methodological consistency between the pre- and post-fire analyses, the study was conducted using only satellite-based remote sensing

data. As ground-based validation was not performed, the precision of the LST estimates may be slightly limited. Statistical significance tests (e.g. *t*-tests or non-parametric alternatives) were not applied, as the focus was on analysing spatial patterns rather than pixel-level variability. Fourthly, the assessment focused on the short-term impacts of the fire, whereas the long-term recovery of vegetation and persistent microclimatic shifts were beyond the temporal scope of the study. Future research could benefit from integrating higher-resolution datasets, in situ observations and extended temporal analyses to provide a more comprehensive evaluation of the impacts of wildfires. Furthermore, integrating atmospheric pollutants data—such as CO, NO_2, and CH_4—into post-fire assessments, as suggested by recent research, could enrich future studies by offering a more comprehensive picture of wildfire-induced environmental changes.

5. Conclusion

The forest fires that occurred in Manavgat, Antalya, Türkiye in the summer of 2021 resulted in vast damage to the vegetation, wildlife, and climate. One undesirable effect is the change in the land cover primarily due to the loss of woodland resulting in temperature increase not only in the incident area but also in the larger region. Such an impact can be analyzed through an evaluation of the LST and UHIER values for pre-incident and the post-incident conditions, using the RS and GIS techniques. A detailed comparison is performed with the Landsat 8 images in 30 m resolution. This study suggests an overall increase in the LST and a decrease in the UHIER, which indicate that losing the tree cover not only has an impact on the forest itself but also the built-up area and the rural area in the close proximity. The decrease in the UHIER should be investigated further since it does not mean the UHIER has been treated, but an increase is evident in the built-up area and the nearby rural area, alike. In order to understand the microclimatic influence of the sea, the study divides the impacted area into two distinct sections; the sea area and the land area. It is concluded that the existence of the large water body has an alleviating role by offsetting the adverse effects of the fire to a certain extent. In conclusion, forest fires have spatially broader effects, but the negative outcomes are more evident in the inner parts of the region and the urban built-up areas. These results underscore the importance of considering coastal proximity and spatial differentiation when assessing post-fire thermal impacts, offering critical insights for urban and regional resilience planning in wildfire-prone areas.

CRediT authorship contribution statement

Mehtap Özenen-Kavlak: Writing – original draft, Visualization, Resources, Methodology, Formal analysis, Data curation, Conceptualization. **Müzeyyen Anıl Şenyel Kürkçüoğlu:** Writing – original draft, Resources, Methodology, Data curation, Conceptualization. **Halil Duymuş:** Writing – original draft, Visualization, Resources, Methodology, Conceptualization. **Gülşah Bilge Öztürk:** Writing – original draft, Formal analysis, Conceptualization. **Saye Nihan Çabuk:** Writing – original draft, Supervision, Resources, Project administration, Methodology, Conceptualization. **Ceren Özcan Tatar:** Writing – original draft, Resources, Conceptualization. **Alper Çabuk:** Writing – review & editing, Writing – original draft, Supervision, Methodology, Conceptualization.

Declaration of competing interest

The authors declare that they have no known competing financial interests or personal relationships that could have appeared to influence the work reported in this paper.

Data availability

Data will be made available on request.

Acknowledgement

This study was supported by the project titled “EPD-NET: Filling the Gap: Development of Ecological Planning and Design Learning Network and Adaptive Smart Training Module for Disaster Resilient and Sustainable Cities” (GAP-101183961), and by the Eskişehir Technical University Scientific Research Projects Commission under Grant No: 23ADP174, 24ADP173, and 25ADP257.

References

Akıncı, H.A., Akıncı, H., 2023. Machine learning based forest fire susceptibility assessment of Manavgat district (Antalya), Turkey. Earth Sci. Inform. 16. https://doi.org/10.1007/s12145-023-00953-5.

de Almeida, C.R., Teodoro, A.C., Gonçalves, A., 2021. Study of the urban heat island (UHI) using remote sensing data/techniques: a systematic review. Environments - MDPI 8.

Antalya Büyükşehir Belediyesi, 2021. Sürdürülebilir enerji eylem planı, Antalya.

Barraza, V., Grings, F., Franco, M., et al., 2019. Estimation of latent heat flux using satellite land surface temperature and a variational data assimilation scheme over a eucalypt forest savanna in northern Australia. Agric. For. Meteorol. 268. https://doi.org/10.1016/j.agrformet.2019.01.032.

Bilgili, E., Coşkuner, K.A., Usta, Y., Sağlam, B., Küçük, O., Berber, T., Göltaş, M., 2019. Diurnal surface fuel moisture prediction model for Calabrian pine stands in Turkey. iForest Biogeosci. For. 12 (3), 262–271. https://doi.org/10.3832/ifor2870-012.

Chen, W., Moriya, K., Sakai, T., et al., 2014. Monitoring of post-fire forest recovery under different restoration modes based on time series Landsat data. Eur. J. Remote Sens. 47. https://doi.org/10.5721/EuJRS20144710.

Çinar, T., Taşpinar, F., Aydin, A., 2024. Analysis and estimation of gaseous air pollutant emissions emitted into the atmosphere during Manavgat and Milas wildfire episodes using remote sensing data and ground measurements. Air Qual. Atmos. Health 17. https://doi.org/10.1007/s11869-023-01463-5.

Çolak, E., Sunar, F., 2020. Spatial pattern analysis of post-fire damages in the Menderes District of Turkey. Front. Earth Sci. 14. https://doi.org/10.1007/s11707-019-0786-4.
Çolak, E., Sunar, F., 2023. Investigating the usefulness of satellite-retrieved land surface temperature (LST) in pre- and post-fire spatial analysis. Earth Sci. Inform. 16. https://doi.org/10.1007/s12145-022-00883-8.
Cristóbal, J., Jiménez-Muñoz, J.C., Prakash, A., et al., 2018. An improved single-channel method to retrieve land surface temperature from the landsat-8 thermal band. Remote Sens. 10. https://doi.org/10.3390/rs10030431.
Cuttelod, A., García, N., Abdul Malak, D., et al., 2008. The Mediterranean: A biodiversity hotspot under threat. In: Vié, J.-C., Hilton-Taylor, C., Stuart, S.N. (Eds.), Wildlife in a Changing World. IUCN, Switzerland, p. 130.
Daniels, L.D., Maertens, T.B., Stan, A.B., et al., 2011. Direct and indirect impacts of climate change on forests: three case studies from British Columbia. Can. J. Plant Pathol. 33. https://doi.org/10.1080/07060661.2011.563906.
Daşdemir, İ., Aydın, F., Ertuğrul, M., 2021. Factors affecting the behavior of large Forest fires in Turkey. Environ. Manag. 67. https://doi.org/10.1007/s00267-020-01389-z.
Duymuş, H., Seyhan, S., Özenen-Kavlak, M., Çabuk, A., 2025. Relationship of urban heat island effect with spatial and temporal changes: a systematic literature analysis. J. Anatolian Environ. An. Sci. 10 (1), 1–14. https://doi.org/10.35229/jaes.1596060.
Gelata, F.T., Jiqin, H., Gemeda, S.C., Asefa, B.W., 2023. Application of GIS using NDVI and LST estimation to measure climate variability-induced drought risk assessment in Ethiopia. J. Water Clim. Chang. 14. https://doi.org/10.2166/wcc.2023.154.
Goldblatt, R., Addas, A., Crull, D., et al., 2021. Remotely sensed derived land surface temperature (Lst) as a proxy for air temperature and thermal comfort at a small geographical scale. Land (Basel) 10. https://doi.org/10.3390/land10040410.
Guangmeng, G., Mei, Z., 2004. Using MODIS land surface temperature to evaluate forest fire risk of Northeast China. IEEE Geosci. Remote Sens. Lett. 1. https://doi.org/10.1109/LGRS.2004.826550.
Heaviside, C., 2020. Urban heat islands and their associated impacts on health. In: Oxford Research Encyclopedia of Environmental Science.
Huang, K., Li, X., Liu, X., Seto, K.C., 2019a. Projecting global urban land expansion and heat island intensification through 2050. Environ. Res. Lett. 14. https://doi.org/10.1088/1748-9326/ab4b71.
Huang, Q., Huang, J., Yang, X., et al., 2019b. Quantifying the seasonal contribution of coupling urban land use types on urban Heat Island using land contribution index: a case study in Wuhan, China. Sustain. Cities Soc. 44. https://doi.org/10.1016/j.scs.2018.10.016.
Hussain, S., Raza, A., Abdo, H.G., et al., 2023. Relation of land surface temperature with different vegetation indices using multi-temporal remote sensing data in Sahiwal region, Pakistan. Geosci. Lett. 10. https://doi.org/10.1186/s40562-023-00287-6.
Jodhani, K.H., Gupta, N., Parmar, A.D., Bhavsar, J.D., 2024a. Synergizing Google earth engine and earth observations for potential impact of land use/land cover on air quality. Results Eng. 22, 102039. https://doi.org/10.1016/j.rineng.2024.102039.
Jodhani, K.H., Patel, D., Madhavan, N., Soni, U., Patel, H., Singh, S.K., 2024b. Channel planform dynamics using Earth observations across Rel River, Western India: a synergetic approach. Spatial Inf. Res. https://doi.org/10.1007/s41324-024-00573-1.
Jodhani, K.H., Patel, D., Valodara, B., Soni, U., Gupta, N., 2024c. Assessment of forest fire severity and land surface temperature using Google earth engine: a case study of Gujarat state, India. Fire Ecol. 20 (1), 23. https://doi.org/10.1186/s42408-024-00254-2.
Junaidi, S.N., Khalid, N., Othman, A.N., et al., 2021. Analysis of the relationship between Forest fire and land surface temperature using Landsat 8 OLI/TIRS imagery. IOP Conf. Series: Earth Environ. Sci.
Kalogiannidis, S., Chatzitheodoridis, F., Kalfas, D., et al., 2023. Socio-psychological, economic and environmental effects of Forest fires. Fire 6. https://doi.org/10.3390/fire6070280.
Karali, A., Varotsos, K.V., Giannakopoulos, C., et al., 2023. Seasonal fire danger forecasts for supporting fire prevention management in an eastern Mediterranean environment: the case of Attica, Greece. Nat. Hazards Earth Syst. Sci. 23. https://doi.org/10.5194/nhess-23-429-2023.
Kavzoğlu, T., 2021. Orman yangınları sebepleri, etkileri, izlenmesi, alınması gereken önlemler ve rehabilitasyon faaliyetleri. Turkish Academy of Sciences, Ankara.
Kırbıyık, B., 2023. Antalya ili hava kalitesinin değerlendirilmesi ve 2021 yılı orman yangınlarının etkisinin araştırılması. Master's Thesis. Konya Teknik Üniversitesi, Konya.
Kolukırık, S., Arslan, D.A., Yılmaz, G.G., 2022. Orman yangınlarının toplumsal etkileri ve görünümü: Medya paylaşımlarında 2021 Büyük Antalya-Manavgat yangını. Afet ve Risk Dergisi 5 (2), 560–580.
Kotroni, V., Cartalis, C., Michaelides, S., et al., 2020. DISARM early warning system for wildfires in the eastern Mediterranean. Sustainability (Switzerland) 12. https://doi.org/10.3390/su12166670.
Kumar, B.P., Babu, K.R., Anusha, B.N., Rajasekhar, M., 2022. Geo-environmental monitoring and assessment of land degradation and desertification in the semi-arid regions using Landsat 8 OLI / TIRS, LST, and NDVI approach. Environ. Challenges 8. https://doi.org/10.1016/j.envc.2022.100578.
Li, C.F., Yin, J.Y., 2013. A study on urban thermal field of Shanghai using multi-source remote sensing data. J. Ind. Soc. Rem. Sens. 41. https://doi.org/10.1007/s12524-013-0268-1.
Liu, W., Wang, S., Zhou, Y., et al., 2010. Analysis of forest potential fire environment based on GIS and RS. In: 2010 18th International Conference on Geoinformatics, Geoinformatics 2010.
Manzo-Delgado, L., Sánchez-Colón, S., Álvarez, R., 2009. Assessment of seasonal forest fire risk using NOAA-AVHRR: a case study in Central Mexico. Int. J. Remote Sens. 30. https://doi.org/10.1080/01431160902852796.
Matin, M.A., Chitale, V.S., Murthy, M.S.R., et al., 2017. Understanding forest fire patterns and risk in Nepal using remote sensing, geographic information system and historical fire data. Int J Wildland Fire 26. https://doi.org/10.1071/WF16056.
Matso, 2023. Manavgat. In: Manavgat Ticaret ve Sanayi Odası. https://www.matso.org.tr/manavgat.html. Accessed 21 Oct 2023.
MGM, 2021. Antalya, Manavgat Station No. 17954 Data. In: Ministry of Environment, Urbanization and Climate Change General Directorate of Meteorology, *Ankara, Türkiye*.
MGM, 2023. İklim sınıflandırması Antalya - Manavgat. In: Ministry of Environment, Urbanization and Climate Change General Directorate of Meteorology. https://www.mgm.gov.tr/iklim/iklim-siniflandirmalari.aspx?m=MANAVGAT. Accessed 21 Oct 2023.
Myers, N., Mittermeler, R.A., Mittermeler, C.G., et al., 2000. Biodiversity hotspots for conservation priorities. Nature 403. https://doi.org/10.1038/35002501.
OBM, 2023. Manavgat Orman İşletme Şefliği. In: Regional Directorate of Forestry. https://antalyaobm.ogm.gov.tr/ManavgatOIM/Sayfalar/default.aspx. Accessed 21 Oct 2023.
Ozenen Kavlak, M., Cabuk, S.N., Cetin, M., 2021. Development of forest fire risk map using geographical information systems and remote sensing capabilities: Ören case. Environ. Sci. Pollut. Res. 28. https://doi.org/10.1007/s11356-021-13080-9.
Özenen-Kavlak, M., Kurtipek, A., Çabuk, S.N., 2020. Coğrafi Bilgi Sistemleri ile orman yangını risk haritası oluşturulması: Ören örneği. Resilience 4. https://doi.org/10.32569/resilience.597887.
Peng, G. xiong, Li, J., Chen, Y. hao, Norizan, A. patah, 2007. A forest fire risk assessment using ASTER images in peninsular Malaysia. J. China Univ. Min. Technol. 17. https://doi.org/10.1016/S1006-1266(07)60078-9.
Rizwan, A.M., Dennis, L.Y.C., Liu, C., 2008. A review on the generation, determination and mitigation of urban Heat Island. J. Environ. Sci. 20. https://doi.org/10.1016/S1001-0742(08)60019-4.
Sajib, M.Q.U., Wang, T., 2020. Estimation of land surface temperature in an agricultural region of Bangladesh from landsat 8: intercomparison of four algorithms. Sensors (Switzerland) 20. https://doi.org/10.3390/s20061778.
Seidl, R., Thom, D., Kautz, M., et al., 2017. Forest disturbances under climate change. Nat. Clim. Chang. 7.
Seyhan, S., 1990. Teke yarımadasının bitki coğrafyası. Doctoral Thesis. Istanbul University.
TOVAG, 2021. Web Tabanlı Yangın Davranışı Tahmin Sistemi (YDTWEB) (TOVAG120O095). The Scientific and Technological Research Council of Türkiye (TÜBİTAK), Project Final Report.

Veraverbeke, S., Verstraeten, W.W., Lhermitte, S., et al., 2012. Assessment of post-fire changes in land surface temperature and surface albedo, and their relation with fireburn severity using multitemporal MODIS imagery. Int. J. Wildland Fire 21. https://doi.org/10.1071/WF10075.

Vlassova, L., Pérez-Cabello, F., Mimbrero, M.R., et al., 2014. Analysis of the relationship between land surface temperature and wildfire severity in a series of landsat images. Remote Sens. 6. https://doi.org/10.3390/rs6076136.

Xu, H.Q., Chen, B.Q., 2004. Remote sensing of the urban heat island and its changes in Xiamen City of SE China. J. Environ. Sci. 16.

Zhang, H., Qi, Z. fang, Ye, X. yue, et al., 2013. Analysis of land use/land cover change, population shift, and their effects on spatiotemporal patterns of urban heat islands in metropolitan Shanghai, China. Appl. Geogr. 44. https://doi.org/10.1016/j.apgeog.2013.07.021.